

# Climate change scenarios at hourly time-step over Switzerland from an enhanced temporal downscaling approach

Adrien Michel<sup>1,2</sup>  | Varun Sharma<sup>1,2</sup> | Michael Lehning<sup>1,2</sup> | Hendrik Huwald<sup>1,2</sup>

<sup>1</sup>School of Architecture, Civil and Environmental Engineering, Ecole Polytechnique Fédérale de Lausanne (EPFL), Lausanne, Switzerland

<sup>2</sup>WSL Institute for Snow and Avalanche Research (SLF), Davos, Switzerland

## Correspondence

Adrien Michel, School of Architecture, Civil and Environmental Engineering, EPFL – Ecole Polytechnique Fédérale de Lausanne, Route Cantonale, Lausanne, Switzerland.

Email: adrien.michel@epfl.ch

## Funding information

Swiss Federal Office for the Environment, Grant/Award Number: 15.0003.PJ/Q102-0785

## Abstract

Many physically-based models for climate change impact studies require sub-daily temporal resolution of the forcing data to provide meaningful predictions. However, climate scenarios are typically available at daily time step, severely limiting the application of such physically-based models. In this study, we propose an enhanced delta-change method for downscaling climate change scenarios from daily to hourly resolution. The approach presented provides objective criteria for assessing the quality of the determined delta and down-scaled time series, while also fixing issues of common quantile mapping methods used for spatial downscaling related to the decrease of correlation between different variables. However, this new approach has limitations in correctly representing statistically extreme events and changes in the frequency of discontinuous events such as precipitation. Smoothing of historical and future data is required prior to applying the delta-change method, and the related parameters are found to have a subtle impact on the correctness of the representation of the seasonal means as well as the resulting (artificial) variability in the scenario data product. This new method is universal and can be applied with smoothing approaches apart from the harmonic fitting used in this work and in the past. In this study, the assessment suggested the use of seven harmonics for the smoothing of the input data as a best choice of this parameter for the data used. The method is applied to a Swiss climate change scenario data set, CH2018, and to a complement of this set to a Swiss alpine measurement network obtained by spatial transfer of CH2018, resulting in a set of 68 climate change scenarios at hourly resolution for 188 stations over Switzerland significantly expanding upon the spatial and temporal resolution of the CH2018 data set. All source code to perform such an analysis and the complete data product are provided open access.

## KEYWORDS

alpine regions, climate change scenarios, delta-change, quantile mapping, Switzerland, temporal downscaling

This is an open access article under the terms of the Creative Commons Attribution-NonCommercial License, which permits use, distribution and reproduction in any medium, provided the original work is properly cited and is not used for commercial purposes.

© 2021 The Authors. International Journal of Climatology published by John Wiley & Sons Ltd on behalf of the Royal Meteorological Society.

## 1 | INTRODUCTION

Climate change scenarios are widely used for impact studies. Many data products do exist, but unfortunately, they do not necessarily meet the required spatial and temporal resolution needed by models used for impact studies. This is the case of the newly released CH2018 scenarios for Switzerland, which are provided only at daily resolution. Here, we present a new version of this data set downscaled at hourly resolution along with an extension of this data set to the Inter-Cantonal Measurement and Information System (IMIS), an Alpine network (IMIS, 2019) of automatic meteorological stations.

The CH2018 climate change scenarios (MeteoSuisse *et al.*, 2018a) consist of future climate data generated by downscaling 68 scenarios produced by the EURO-CORDEX project using the ‘quantile mapping’ (QM) approach. This method consists of building a one-to-one functional mapping between quantiles of distributions of measured and simulated data sets. This mapping is derived for a reference period and applied to simulated future climates to generate data at the point of measurement. This technique is used in CH2018 to perform spatial downscaling from RCM grid data to point stations. This is also used in this study to perform spatial transfer between CH2018 scenarios and the alpine IMIS station network. CH2018 is a significant improvement over the previous generation of scenarios released for Switzerland, CH2011 (CH2011, 2011), in terms of methodology as well as number of stations, in addition to being based on the latest climate model outputs. However, the new data sets are still limited in that they only provide future climate scenarios at daily time scale. Moreover, since the QM methodology is applied separately for each station as well as for each variable, there is no guaranteed spatio-temporal consistency between variables and between stations.

Our motivation in expanding the CH2018 data sets from daily to hourly timescales along with additional stations arises from requirements in two independent projects, namely the Hydro-CH2018 project (FOEN, 2018) of the Swiss Federal Office for the Environment, and the Climate Change Impacts on Alpine Mass Movements (CCAMM) (CCAMM, 2019) research program of the Swiss Federal Institute for Forest, Snow and Landscape Research (WSL). The Hydro-CH2018 project aims at assessing the impact of expected climate changes on the hydrological system in Switzerland. The CCAMM project investigates the influence of climate change on avalanche danger as well as other mass movements such as rockfalls and landslides. Both projects use models that require hourly input data.

While spatial downscaling has been extensively discussed in the literature, temporal downscaling has

received much less attention. Temporal downscaling can be performed through dynamical downscaling and statistical downscaling (SD) methods. Since this application is done on RCMs output, we focus here only on SD methods. The main methods used in temporal SD include the *delta-change* method (also called *change factor* method), and weather generators (WG).

In the delta-change approach (discussed for example, in Anandhi *et al.* (2011)), first the difference or ratio (delta) between measurements over a reference period in the past and the output of a climate change scenario over a given period, both at daily resolution, is computed. Then, this delta is applied to a past time series at hourly resolution to obtain an hourly time series for the future period encapsulating the main annual and seasonal behaviour of the output of the climate change scenario over this period. The second approach relies on WG (see for example, Peleg *et al.* (2019)). In this method, some statistical moments (mean, variance, skewness, etc.) are computed for historical time series. Then, a transient factor of change of these moments is computed between historical data and future time series from scenarios. Finally, some new time series are generated for the future by randomly picking values from distributions having statistical moments adapted at this point in time using the computed factor of change.

Weather generators require significant calibration and existing 2-dimensional generators for Switzerland have been calibrated only for a few regions (Peleg *et al.*, 2017). This prevents their use in our applications. As a consequence, we go back to the delta-change approach used in the previous CH2011 scenarios detailed in the work of Bosshard *et al.* (2011) and further develop it, especially regarding the assessment of the quality of the time series obtained and the validation of the parameters used. Indeed, by investigating time series obtained from the former method, it became evident that it does not necessarily represent correctly the seasonal cycle of the climate change scenario. In addition, this method has been originally developed and validated only for precipitation and temperature, while it has been used for other variables without any further validation (e.g., case study in CH2018).

In the present study, we provide temporally down-scaled time series for precipitation and temperature, as well as for relative humidity, incoming shortwave solar radiation and wind speed. The obtained time series are used in a case study. The aim of this case study is not to discuss impact of climate change, but to illustrate, for realistic ‘end-user’ applications, the difference induced by the choice of the inner parameters of the delta-change method. In addition to providing new climate change data sets, the main objective of this work is to propose

new metrics for assessing the quality of downscaled time series in order to choose the right parameters for the downscaling process.

The QM is applied to 198 IMIS stations in order to obtain daily climate change time series since IMIS stations have not been included in the original CH2018 data set. The time series are downscaled at hourly resolution at decadal intervals for 72 MeteoSwiss stations and 116 IMIS stations where the requirements for applying the delta method are met. They are also downscaled at hourly resolution at 30-years intervals for 58 MeteoSwiss stations (when sufficient historical data is available). All time series are publicly available with relevant metadata for end users, and all the source codes and detailed instructions on how to use this method on different data sets are provided along with this work.

## 2 | DATA

### 2.1 | MeteoSwiss data

Part of the meteorological data used in this paper are measurements from the MeteoSwiss (MCH) automatic monitoring network which are distributed through IDAWEB (2019). Data at daily and hourly resolution for 2-m air temperature, precipitation accumulation, wind velocity, relative humidity and incoming shortwave solar radiation are used.

### 2.2 | IMIS data

The second part of the meteorological data are acquired through the IMIS automatic monitoring network (IMIS, 2019), comprising of 198 automatic weather stations well spread over the Swiss Alps, operated by the WSL Institute for Snow and Avalanche Research, SLF. This network features two types of stations, so-called 'wind' and 'snow' stations. While wind stations provide wind speed (7.5 m), gust speed, wind direction, air temperature (2 m) and relative humidity, the snow stations provide the following additional measurements: snow height, reflected shortwave radiation, snow temperature at 25, 50 and 100 cm above ground, infrared snow surface temperature. Some stations also have a (non-heated) rain gauge for liquid precipitation. For stations without heated rain gauge, the snow cover model SNOWPACK (Lehning *et al.*, 2002) is used to retrieve the snow precipitation from snow height measurements, and during snow-free seasons precipitation is obtained by extrapolating precipitation measured at nearby MCH stations.

In SNOWPACK, incoming shortwave solar radiation can be computed from the reflected shortwave radiation and the surface albedo. While this method is well suited for winter, when the ground is snow-covered, it gives poor results in summer. For this reason, incoming shortwave radiation was excluded from the present downscaling for IMIS stations.

IMIS stations are not included in the CH2018 data set. The first step with these time series is thus to produce climate change scenario output using the quantile mapping method for spatial transfer, as described in Section 2.4.

### 2.3 | CH2018 climate change scenarios

The CH2018 scenarios (MeteoSuisse *et al.*, 2018b) are based on the European Coordinated Regional Climate Downscaling Experiment, EURO-CORDEX. In EURO-CORDEX, regional climate models (RCM) are used to dynamically downscale the global climate model simulations from the Coupled Model Intercomparison Project CMIP5 (Taylor *et al.*, 2012). Both EUR-11 (0.11°, ~12.5 km) and EUR-44 (0.44°, ~50 km) spatial resolutions of EURO-CORDEX are used in CH2018. Note that both EUR-11 and EUR-44 resolutions can be used for the same GCM-RCM chain. For more details, see MeteoSuisse *et al.* (2018a).

These data are provided at daily time steps at the locations of the MCH automatic weather station. Available variables are the 2 m air temperature and relative humidity, daily minimum and maximum air temperature, near surface 10 m wind speed, precipitation, and incoming shortwave radiation. There are 68 model chain outputs: 31 for the business-as-usual 'Representative Concentration Pathways' RCP8.5 scenario, 25 for the intermediate case RCP4.5, and 12 for an ambitious mitigation pathway RCP2.6.

### 2.4 | Quantile mapping on IMIS data

The quantile mapping technique used to generate the CH2018 data set is limited to MCH stations. Using the methodology of Rajczak *et al.* (2016), the future climate scenarios are spatially transferred from the MCH station network to the IMIS stations for air temperature, precipitation, wind speed and relative humidity. The methodology is detailed in this Section. Firstly, for each IMIS station, the 'most representative station' (MRS) of the MCH network is found using correlation values between the IMIS station and each station in the MCH network (for which CH2018 data sets are available).

The bias-corrected climate scenarios at the MRS are spatially transferred to the corresponding IMIS station using the quantile mapping (QM) approach. The transfer function required to perform the QM is generated using historical observations available at both the MRS and the IMIS station. Note that this differs from the QM technique employed in CH2018 where the climate change signal is being transferred from a climate model output to a local station. Thus, in the context of CH2018, the intended implication of the QM technique was to perform bias correction alone. Using QM to spatially transfer information between observational data sets is also termed as ‘empirical quantile mapping’ in the literature. More related information can be found in Maraun (2016) and Maraun *et al.* (2017).

Performing only the spatial transfer between two measurement stations has two implications. Firstly, since the transfer function is being built using ‘real’ observations at both the MRS and the IMIS stations, time series of a limited number of years, is generally sufficient as opposed to the climate model-to-station transfer function in CH2018, where 30 years of measurements are necessary. The longer time series in this case are required since the QM must correct for model errors as well as spatial transfer. The validity of using shorter time series for station-to-station transfer was confirmed in the detailed checks by Rajczak *et al.* (2016).

In fact, it is due to this very constraint that the CH2018 scenarios are available for considerably fewer stations than the entire MCH station network. Secondly, the periods of observational time series do not necessarily need to be contained in the ‘historical’ period defined by the CMIP5/CORDEX climate simulations, and thus the most up-to-date observational time series can be used to develop the spatial transfer function. The spatial transfer function is assumed to be valid in past, current and future climates (which corresponds to the commonly assumed stationary hypothesis). This is one important limitation of this method and is further discussed in Section 5.1.

The QM-based spatial transfer is performed for all IMIS stations resulting in future climate scenarios for 198 stations in addition to those in the CH2018 data set.

## 2.5 | Variables, stations, and periods used

The temporal downscaling is applied to all the variables available in the CH2018 data set: Air temperature (TA), precipitation (PSUM), relative humidity (RH), wind speed (VW) and total incoming shortwave radiation

(ISWR), the latter not for IMIS stations as discussed in Section 2.2.

Stations where the downscaling is performed are shown in Figure 1. A complete list of stations, together with the variables downscaled, is presented in Tables S1–S6. The reasons for excluding some stations are detailed in Section S3.

The time series are downscaled to 10-year periods (all decades between 1990 and 2100) using the period 2005–2015 for historical measurements. When sufficient data are available, time series are also downscaled to 30-years periods (1980–2010, 2010–2040, 2040–2070, and 2070–2100) using the reference period 1985–2015 of historical measurements. Periods including historical measurements are referred to as ‘historical time series’, while periods for which downscaling is applied are referred to as ‘climate change time series’ or ‘future time series’, even if part of these periods are in the past.

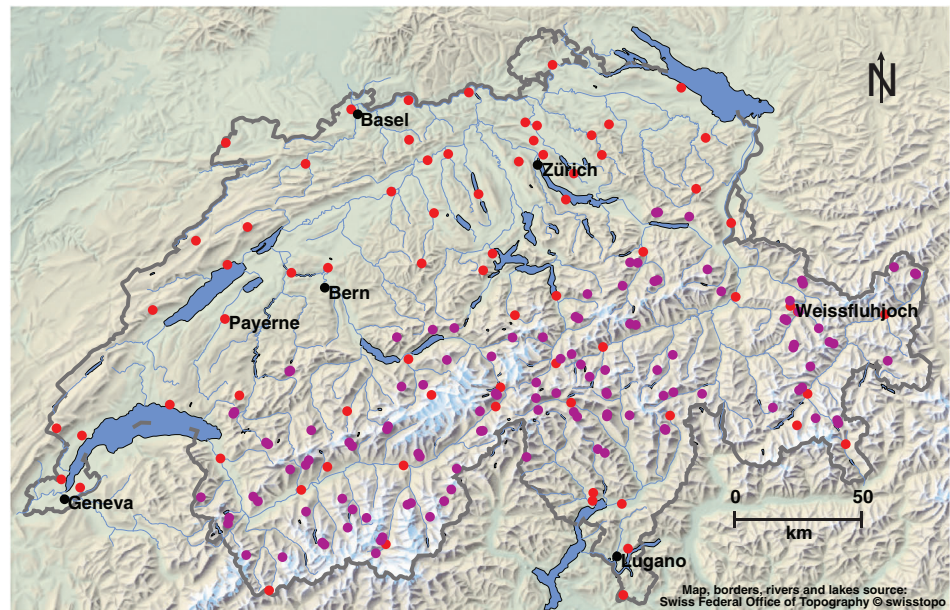
## 3 | DELTA COMPUTATION METHOD

The method developed in this paper is an improvement of the method described in MeteoSuisse *et al.* (2018a), section 10.2, in CH2011 (2011), section 2.7 and A2, and in Bosshard *et al.* (2011). A drawback of the method of Bosshard *et al.* (2011) is that seasonal means are not well represented in downscaled time series, which is corrected here by assessing the quality of the delta leading to a better choice of parameters.

A definition of the delta is, for each variable, an additive or multiplicative factor that will be used to modify historical hourly time series in a way that the mid- and long-term means (seasonal, yearly) are as close as possible to the climate change daily time series to be downscaled, without adding any natural variability. Additive delta is used for temperature while multiplicative delta is used for other variables. Note that multiplicative delta might lead to unrealistically high values; this effect is discussed in Section 5.1.

The flow chart shown in Figure 2 describes the whole methodology while this section describes only the steps presented in the orange box of the flow chart. A simple method to obtain the delta would be to subtract or divide the daily value averaged over all years from climate scenarios to the one obtained from historical periods. However, the delta obtained exhibits significant noise. Even by averaging each day of the year (DOY) over many years, some variability remains in the data, which is undesirable in this case (see Figure 3 bottom-left panel). Indeed, natural variability is already present in the historical time series. If some high

**FIGURE 1** Map showing the location of the MeteoSwiss stations (red) and IMIS stations (purple) where the temporal downscaling is applied [Colour figure can be viewed at [wileyonlinelibrary.com](http://wileyonlinelibrary.com)]



frequency variability remains in the delta, artificial variability will be added when applying the delta to historical time series.

For variables such as precipitation, with high intermittency (many zero values), smoothing of the data is mandatory. Even with a DOY averaging, some days show very low amounts of precipitation (see Figure 3 top panels), leading to arbitrary high or low delta values, and thus potentially unrealistically high precipitation events. In addition, a statistical artefact will lead to higher delta values when the time series used to compute the delta are uncorrelated. As a consequence, the mean of the historical time series when the delta is applied (the downscaled time series) will be larger than the mean of the climate change time series. Smoothing the time series beforehand allows to significantly reduce the impact of this artefact. Note that these two issues impose a smoothing of the time series themselves before the computation of the delta instead of smoothing of the delta. A related extensive discussion is given in (Bosshard *et al.*, 2011).

The simplest approach to smooth the data is a running mean. However, a running mean applied to a time series with a sinusoidal shape, as air temperature for instance, tends to flatten the amplitude and the seasonal mean in summer and winter will be affected. Another solution, proposed in Bosshard *et al.* (2011), is to approximate the time series with an harmonic function, which is actually a truncation until the  $n$ th term of the discrete Fourier transform (Storch and Zwiers, 1999; CH2011, 2011).

Given a periodic discrete time series  $x = [x_1, \dots, x_T]$ , it can be approximated by a superposition of sine and cosine functions of various frequencies:

$$x_t = a_0 + \sum_{j=1}^{T-1} a_j \cos(2\pi\omega_j t) + b_j \sin(2\pi\omega_j t) \quad (1)$$

where:

$$\omega_j = \frac{j}{T} \quad (2)$$

$$a_0 = \frac{1}{T} \sum_{t=1}^T x_t = \bar{x} \quad (3)$$

$$a_j = \frac{2}{T} \sum_{t=1}^T x_t \cos(2\pi\omega_j t) \quad (4)$$

$$b_j = \frac{2}{T} \sum_{t=1}^T x_t \sin(2\pi\omega_j t) \quad (5)$$

In Equations (1) and (2),  $j$  is the current harmonic number and its value corresponds to the frequency; here we also call  $j$  the smoothing parameter. In this application, the objective is to approximate the time series by using only low frequency terms (seasonal components), ignoring the high frequency terms (natural variability), which means stopping the sum in (1) at some value of  $j$ . Bosshard *et al.* (2011) found that ending at  $j = 3$  yields the best value for precipitation, but this assessment is only based on testing that no additional natural variability is added to the final time series. Contrary to the statements in the CH2011 report (CH2011, 2011) we show that this method does actually not preserve the

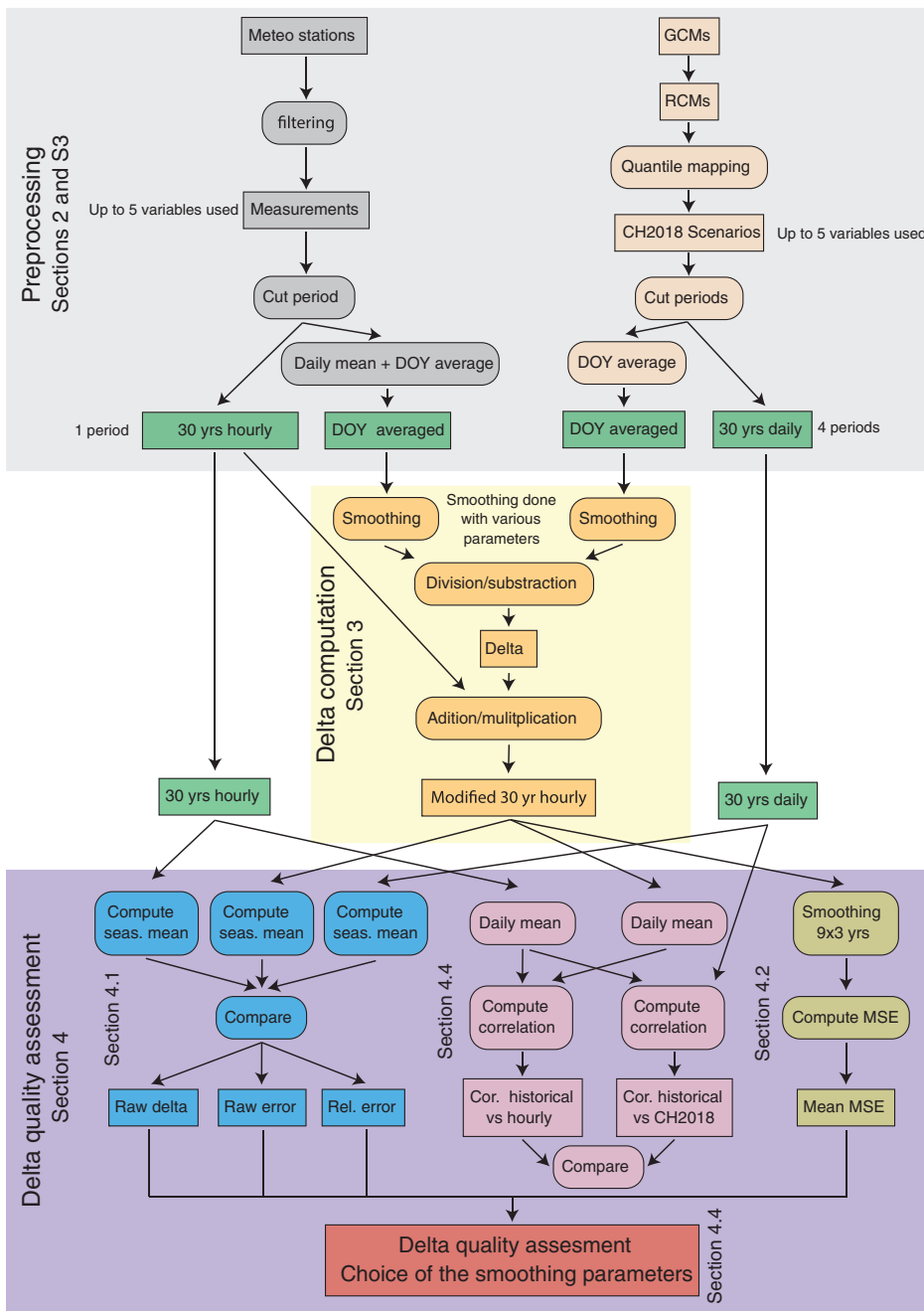


**FIGURE 2** Schematic of the method. Rounded boxes represent operations, while squared boxes represent time series or data. The various steps presented in this flow chart are explained in detail in the text [Colour figure can be viewed at [wileyonlinelibrary.com](http://wileyonlinelibrary.com)]

seasonal means. Figure 4 top panels shows the delta obtained with  $j = 3$  for temperature at the Payerne station.

A better agreement for seasonal means can be achieved by increasing the number of harmonics used. Figure 4 bottom panels shows the results for  $j = 7$ . The drawback is that the obtained delta is more noisy and thus some natural variability might be added.

In the present method, we keep the same smoothing approach as in Bosshard *et al.* (2011), but the metrics for assessing the quality of the delta and the choice of the

smoothing parameter is enhanced. The assessment method presented below is not dependent on the smoothing approach chosen and can thus be applied with any smoothing function.

## 4 | DELTA QUALITY ASSESSMENT

This section describes the elements of the purple part of the flow chart (Figure 2). The impact of the smoothing parameter is assessed in terms of seasonal mean

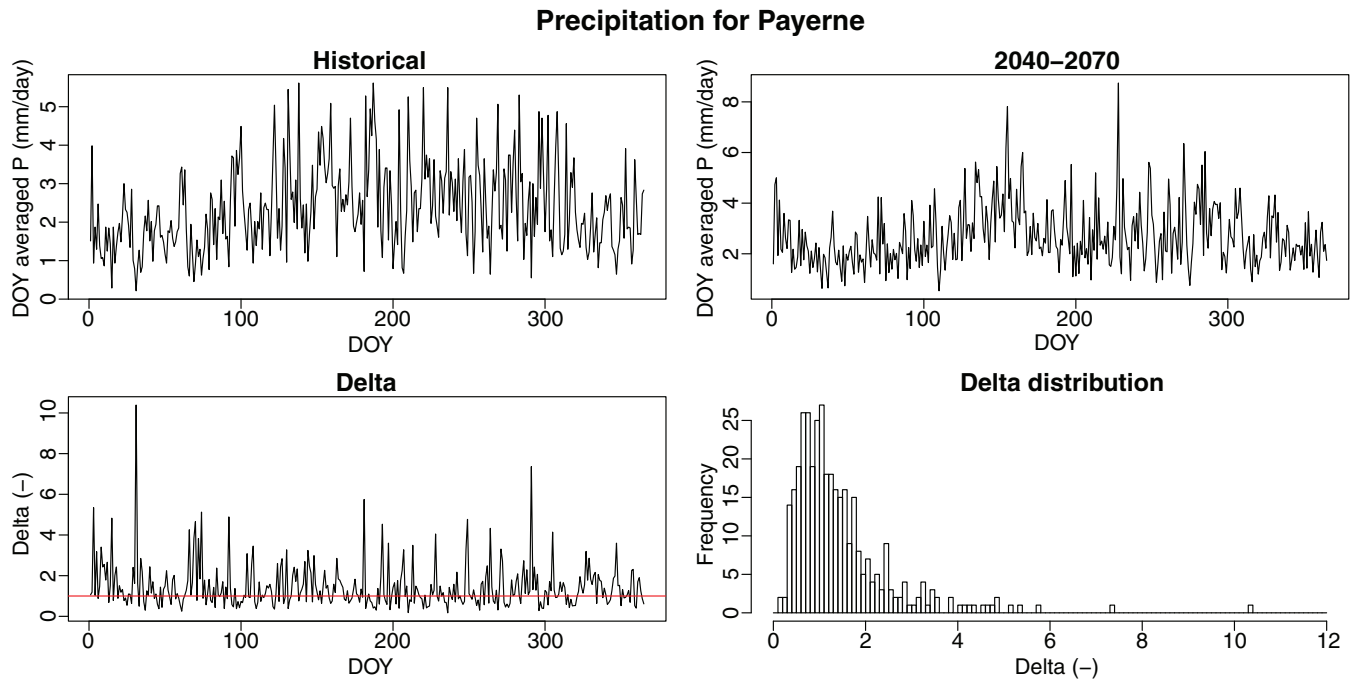


**FIGURE 3** Top left: DOY-averaged time series for precipitation from historical data (1985–2015). Top right: DOY-averaged precipitation from CH2018 model chain output DMI-HIRHAM\_ECEARTH\_EUR11\_RCP85 for the period 2040–2070. Bottom left: Delta obtained by dividing the model DOY-averaged model output by historical data. The red line represents the mean value. Bottom right: Distribution of delta values [Colour figure can be viewed at [wileyonlinelibrary.com](http://wileyonlinelibrary.com)]

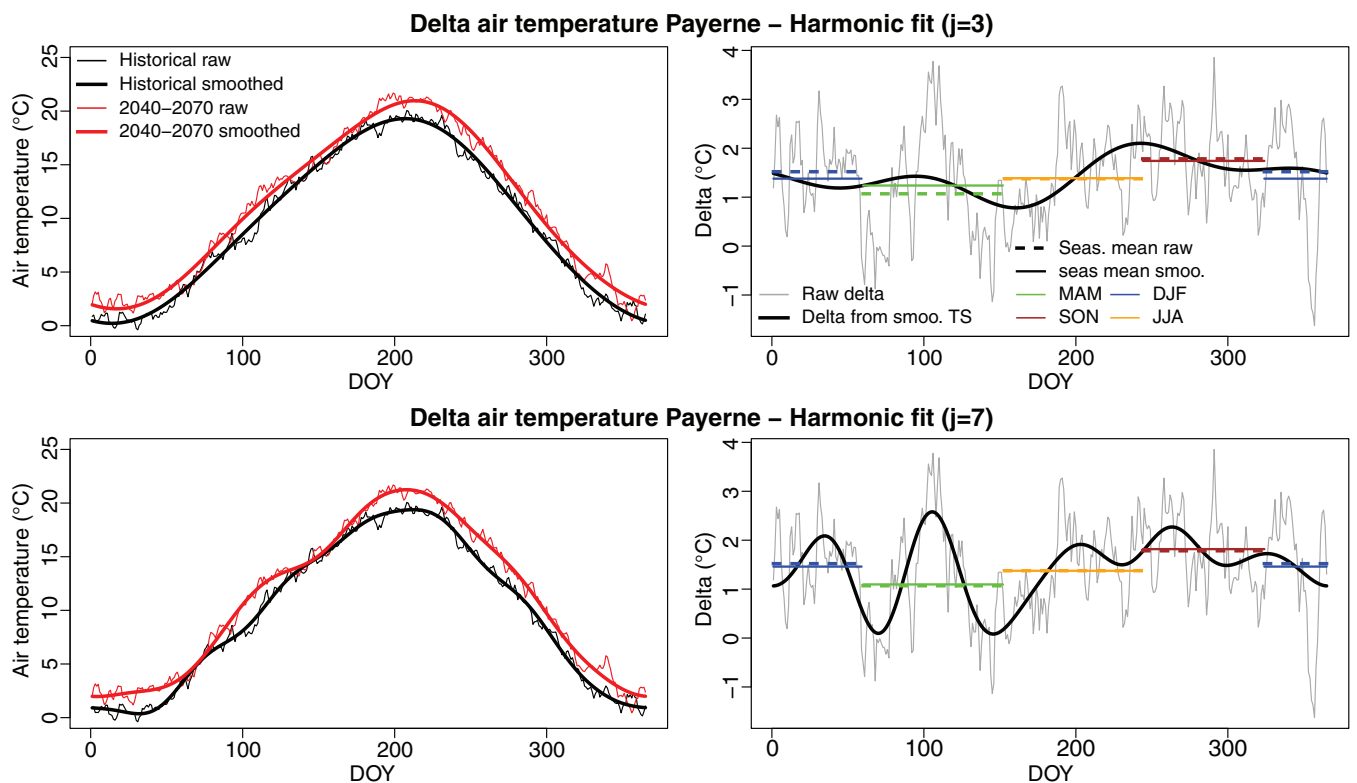


**FIGURE 4** Left: 1-year-averaged temperature for historical measurements for the period 1985–2015 (thin black) and CH2018 model chain DMI-HIRHAM\_ECEARTH\_EUR11\_RCP85 for the period 2040–2070 (thin red). Thick lines indicate smoothing obtained with an harmonic fitting with  $j = 3$ . Right: Delta obtained by subtracting the raw data (thin black line) and the smoothed data (thick black lines). Coloured lines represent seasonal means, with solid lines being the mean of delta from smoothed time series, and dashed lines the mean of delta obtained with raw data [Colour figure can be viewed at [wileyonlinelibrary.com](http://wileyonlinelibrary.com)]

and natural variability. In addition, we show how this method restores the inter-variable and inter-station correlations, which might be reduced by the fact that the QM used for spatial downscaling and spatial transfer is applied separately for each station and for each variable..

#### 4.1 | Seasonal mean conservation

Section 3 showed the importance of smoothing the time series to preserve, as much as possible, the seasonal means, without including much additional natural variability. For air temperature, it is easy to compare the seasonal mean of the delta obtained from raw data and from smoothed data, as shown in Figure 4, for assessing whether the seasonality is conserved. However, for precipitation, as discussed in Section 3, the delta obtained from raw data is rather meaningless and thus it cannot be compared to the delta obtained from smoothed data. To assess the ability of the method to capture correctly the seasonal means, the following approach is proposed (blue elements in the purple parts of the flow chart Figure 2).

The delta between historical and CH2018 time series is computed and applied to the whole historical time series. Then, the seasonal means of the modified time series are computed and compared to the seasonal means of the raw CH2018 scenario and to the historical data. In other words, instead of comparing the smoothed delta with the delta from the raw data, we compare the application of the delta to time series with the raw time series themselves, which also allows to see any bias introduced by the application of the delta.

By defining:

- $\bar{V}_S^H \equiv$  Mean of historical data for the variable  $V$  and the season  $S$
- $\bar{V}_S^{CC} \equiv$  Mean of CH2018 data for the variable  $V$  and the season  $S$
- $\bar{V}_S^{\Delta H} \equiv$  Mean of the downscaled time series, that is, historical data with the delta applied, for the variable  $V$  and the season  $S$ ,  
we can further define:
- $\Delta V_S^{CC} \equiv \bar{V}_S^{CC} - \bar{V}_S^H$ , the difference between CH2018 and historical seasonal mean, that is, the raw seasonal climate change signal from climate change scenario, for the variable  $V$  and the season  $S$ .
- $\Delta V_S^{DS} \equiv \bar{V}_S^{CC} - \bar{V}_S^{\Delta H}$ , the difference between the temporally downscaled time series and the CH2018 seasonal mean, that is, the raw error on seasonal mean of the reconstructed time series compared to raw climate change data, for the variable  $V$  and the season  $S$ .

- $\Delta V_S^{rel} \equiv \frac{\Delta V_S^{DS}}{\Delta V_S^{CC}}$ , the relative error of the downscaled time series seasonal mean compared to the raw delta signal, for the variable  $V$  and the season  $S$ .

The last two values allow for assessing the quality of the delta in terms of preserving the seasonal means. Note that in Figure 4 the quality of the delta itself is assessed, whereas now the quality of the delta applied to the historical data can be assessed, which is, in the end, the value of interest. The graphical output of this assessment method is shown in Figure 5. Note that this figure is based on only one scenario and one time period.

To optimally infer the impact of the number of harmonics used, the procedure needs to be applied to all model chain outputs and all periods. Figures 6 and 7 show the output for Payerne for air temperature and precipitation, for the 56 model chains, the four 30-years time periods used, and for two values of  $j$ , namely 3 and 7. The three other variables analogue plots for the alpine station of Weissfluhjoch are shown in Figures S1–S8.

This analyse shows that:

- The raw error  $\Delta V_S^{DS}$  is almost the same for each time period and is not strongly correlated to the strength of the signal  $\Delta V_S^{CC}$ . As a consequence, there is also no correlation between the raw error and the RCP scenario.
- Increasing the number of harmonics (from  $j = 3$  to  $j = 7$ ) does reduce the error by roughly a factor of 2.
- The absolute error is strongly dependent on the season, but increasing the number of harmonics decreases the seasonal dependence of the error.

#### 4.2 | Natural variability

Increasing  $j$  leads to an improved representation the seasonal cycle, as discussed in the previous section, but it increases artificially the variability simultaneously.

To assess this effect, an approach similar to Bosshard *et al.* (2011) is used (green elements in the purple part of the flow chart Figure 2). The 30 years periods are split into 10 periods of 3 consecutive years. Then, 9 out of the 10 periods are DOY averaged and used to compute the harmonic factors and obtain a smoothed time series. This smoothed time series is compared to the DOY average of the remaining 3 years and the root mean square error (RMSE) between them is computed. This is repeated 10 times (changing the 3 years verification period) and the 10 RMSE values are averaged. The method is applied to various  $j$  values while trying to minimize the RMSE. Figure 8 shows the result of this method. The output for temperature and precipitation are similar to the Bosshard *et al.* (2011) results. Despite an increase of the mean



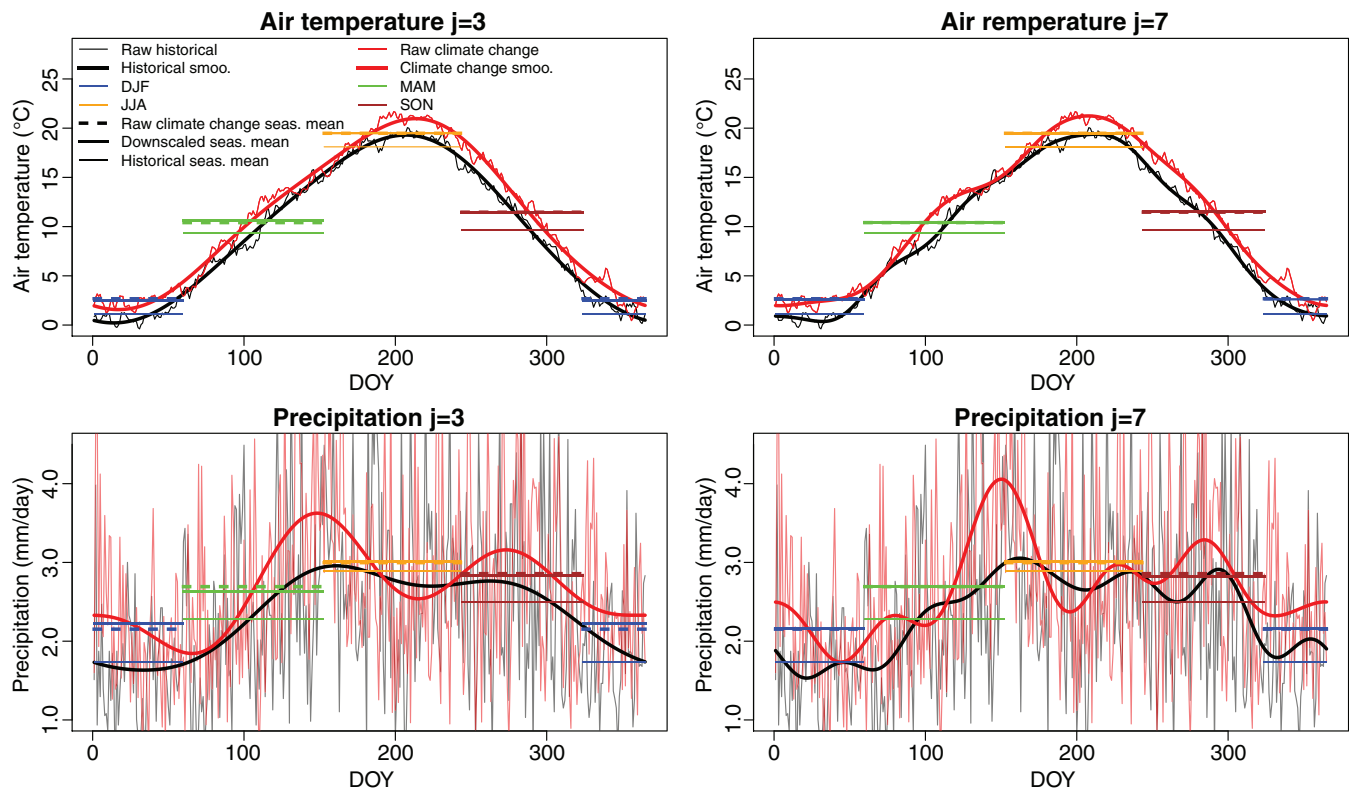


**FIGURE 5** Top: Raw (thin line) and smoothed (thick line) air temperature data for the measured historical period 1985–2015 (black), and for the CH2018 model chain DMI-HIRHAM\_ECEARTH\_EUR11\_RCP85 for the period 2040–2070 (red). Smoothing is obtained by harmonic fitting with  $j = 3$  (left) and  $j = 7$  (right). Coloured lines represent the seasonal mean for period 2040–2070 (dashed lines), for historical measured time series with delta applied (thick solid lines), and for raw historical measured time series (thin solid lines). Bottom: Same for precipitation [Colour figure can be viewed at [wileyonlinelibrary.com](http://wileyonlinelibrary.com)]

RMSE value when  $j$  increases, the increase is very small compared to the variability between the various model chains (top row). In an attempt to remove the variability between model chains and highlight the influence of the chosen harmonic value, the second row of Figure 8 shows the same output as the top row but for each model chain the mean of the RMSE for all  $j$  values is subtracted separately. We refer to this value as centred RMSE.

In the third row of Figure 8, the RMSE is plotted against the time period, to show that there is no correlation between the RMSE and the time period used, as we can expect. A similar figure for the station Weissfluhjoch is shown in Figure S9, exhibiting the same general behaviour.

### 4.3 | Final assessment

The goal is to minimize simultaneously, and for each variable, the following two objective functions: the mean centred RMSE, and the mean absolute seasonal raw error, presented in Sections 4.2 and 4.1, respectively. The mean absolute seasonal raw error is obtained by averaging the absolute values of the raw error for all

model chain outputs, all periods, and all seasons for a given variable and harmonic smoothing value, that is, averaging the absolute values of all the points of Figure 6 left panel. The mean centred RMSE is obtained by taking the mean of the centred RMSE values for all scenarios and periods (i.e., the mean of each box in the second row of Figure 8).

Figure 9 shows values of the two objective functions for all five variables at the Payerne and the Weissfluhjoch stations. The error bars in the plots correspond to the variance of the data. Additional stations are shown in Figures S10–S68. Since the two objective functions have different magnitudes, and since it is difficult to deduce a physical significance of the mean RMSE, it is not possible to define a real metric in the ‘mean MSE – mean absolute seasonal’ error space. In addition, the problem being driven by only one variable,  $j$ , this problem cannot be solved by a Pareto Front approach. Indeed, the curve drawn by the points in Figure 9 is already the Pareto Front. Therefore, it is proposed to perform the analysis graphically.

An analysis of the plots obtained for a subset of 20 MCH stations over 30 years and 10 years and 20 IMIS

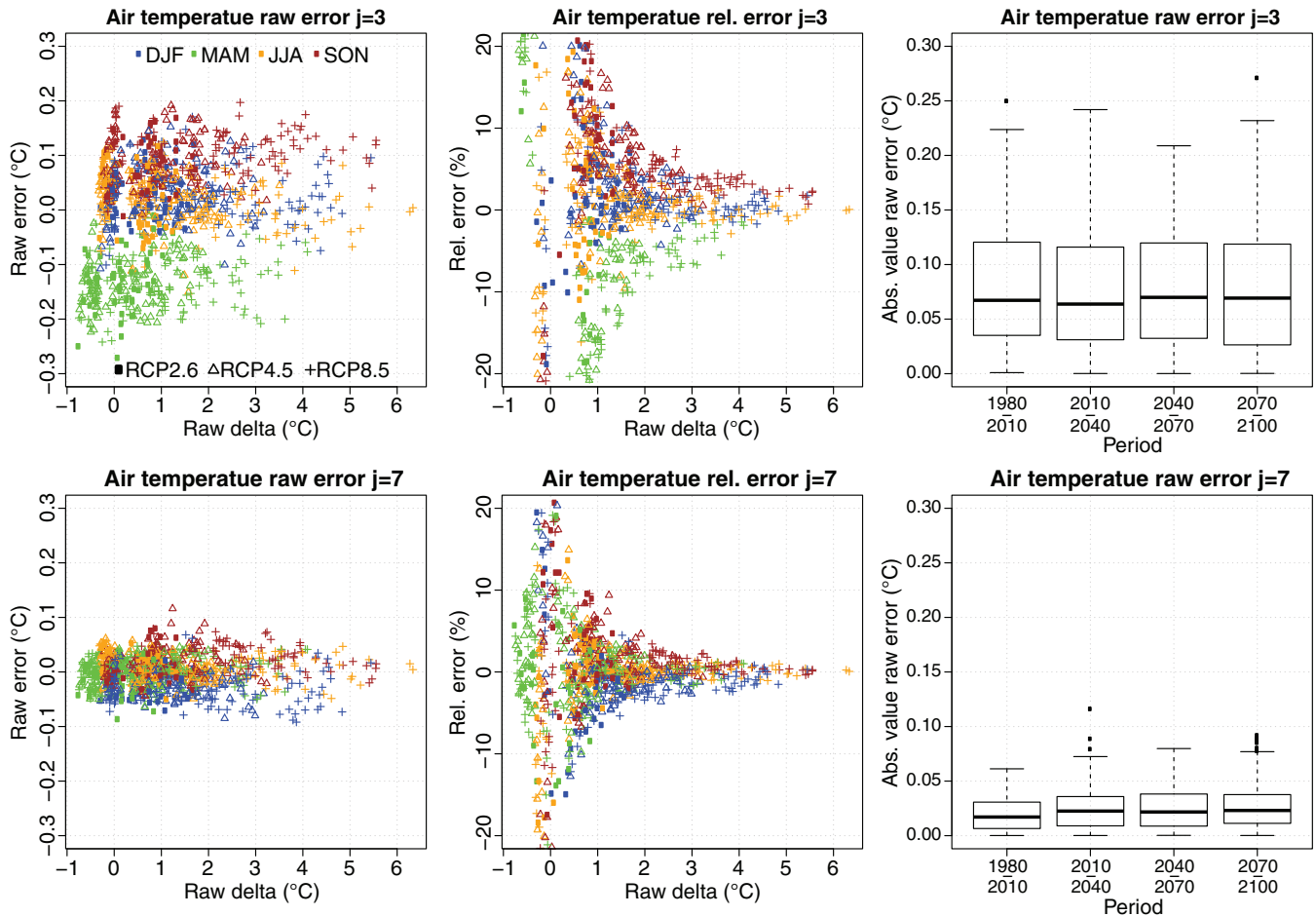


**FIGURE 6** Left 2 panels: Air temperature seasonal absolute and relative error ( $\Delta_A V_S^A$  and  $\Delta_R V_S^A$ ) plotted as a function of the raw delta values ( $\Delta V_S^{CC}$ ) for the station Payerne. Colours indicate season and symbols indicate the RCP scenario. Right panel: Box plot of the seasonal absolute error  $\Delta_A V_S^A$  (absolute value) for the four time periods. Top: Harmonic smoothing with  $j = 3$ . Bottom: Harmonic smoothing with  $j = 7$  [Colour figure can be viewed at [wileyonlinelibrary.com](http://wileyonlinelibrary.com)]

stations over 10 years show that the smoothing parameter  $j$ , which best keeps both sources of errors low is equal to 7. This value is then further used to produce the down-scaled time series.

We emphasize that the best value found here is probably dependent on the data set used. In other applications, especially with data from a climatic regime different from the mid-latitude climate of the Swiss Plateau or the climate in the Swiss Alps, a similar assessment should be performed in order to define the best smoothing parameter value.

#### 4.4 | Inter-variable correlation

The spatial downscaling applied in CH2018 using the QM method, and the similar approach used to obtain climate change scenarios at IMIS station locations (Section 2.4), reduce the temporal correlation between

variables and the spatial correlation between stations. The former is problematic for physically based models. It is shown below that, as a side-effect, the temporal downscaling method allows for eliminating these issues. This section corresponds to the pink elements in the purple part of the flow chart (Figure 2).

To infer the impact of the QM and delta-change downscaling on inter-variable correlations at a single station, correlation is computed between variables for the historical time series, but also for each scenario using raw CH2018 data and downscaled time series (results shown here uses  $j = 7$  for the delta computation, but results with other  $j$  values are similar). These correlations are computed over the historical period only (1980–2010) to allow for comparison with historical data, and are averaged over all scenarios. Figure 10 shows such correlations for the stations Payerne and Weissfluhjoch. For raw CH2018 and hourly downscaled time series, the variance of the correlation value between scenarios is also shown

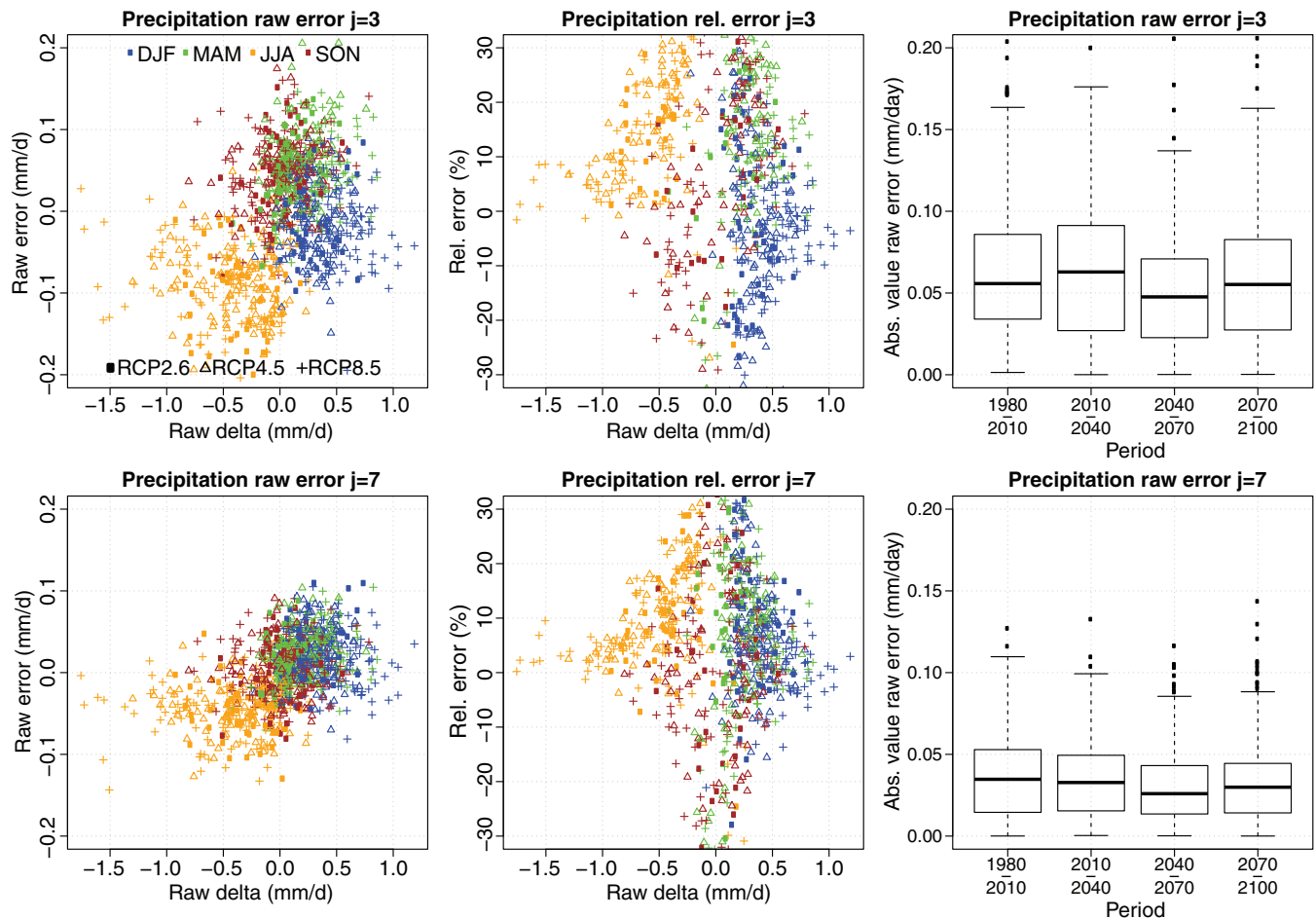


**FIGURE 7** Left 2 panels: Precipitation seasonal absolute and relative error ( $\Delta_A V_S^\Delta$  and  $\Delta_R V_S^\Delta$ ) plotted as a function of the raw delta values ( $\Delta V_S^{CC}$ ) for the station Payerne. Colours indicate season and symbols indicate the RCP scenario. Right panel: Box plot of the seasonal absolute error  $\Delta_A V_S^\Delta$  (absolute value) for the four time periods. Top: Harmonic smoothing with  $j = 3$ . Bottom: Harmonic smoothing with  $j = 7$  [Colour figure can be viewed at [wileyonlinelibrary.com](http://wileyonlinelibrary.com)]

(panels c, e, h and j). Differences in the correlations are observed between historical and raw CH2018 time series (compare panel a to panel b and panel f to panel g), while for temporally downsampled time series the correlation pattern is very close to the historical one (compare panel a to panel d and panel f to panel i). In addition, there is an important spread of the correlation values between scenarios for raw CH2018 (as illustrated by the variance plots; note that the scale is different between raw CH2018 and downsampled data, in order to distinguish differences in downsampled correlation variance). This implies that for some scenarios, the deviation from the observed correlation over historical time series is even more pronounced. This spread is not observed in time series downsampled with the delta-change method.

A similar approach is used to compare variables between stations. Two pairs of relatively close stations are chosen, here the pair Basel Binningen – Zürich Kloten and the pair Chur – Davos. The correlation between identical variables are computed between the

two stations for each pair, again using historical, raw CH2018 and temporally downsampled time series, all the scenarios and the period 1980–2010. Results are shown in Figure 11 and similar behaviour as for the inter-variable correlation is observed.

From these two comparisons, it is concluded that the lack of correct inter-variable and inter-station correlation in the CH2018 data set is improved by the temporal downscaling.

## 5 | LIMITATIONS OF DELTA-CHANGE METHOD AND RESULTING DATA SET

### 5.1 | General considerations

The CH2018 data set comes with some limitations and pitfalls, mostly induced by the use of quantile mapping. The main points are presented in this section while full

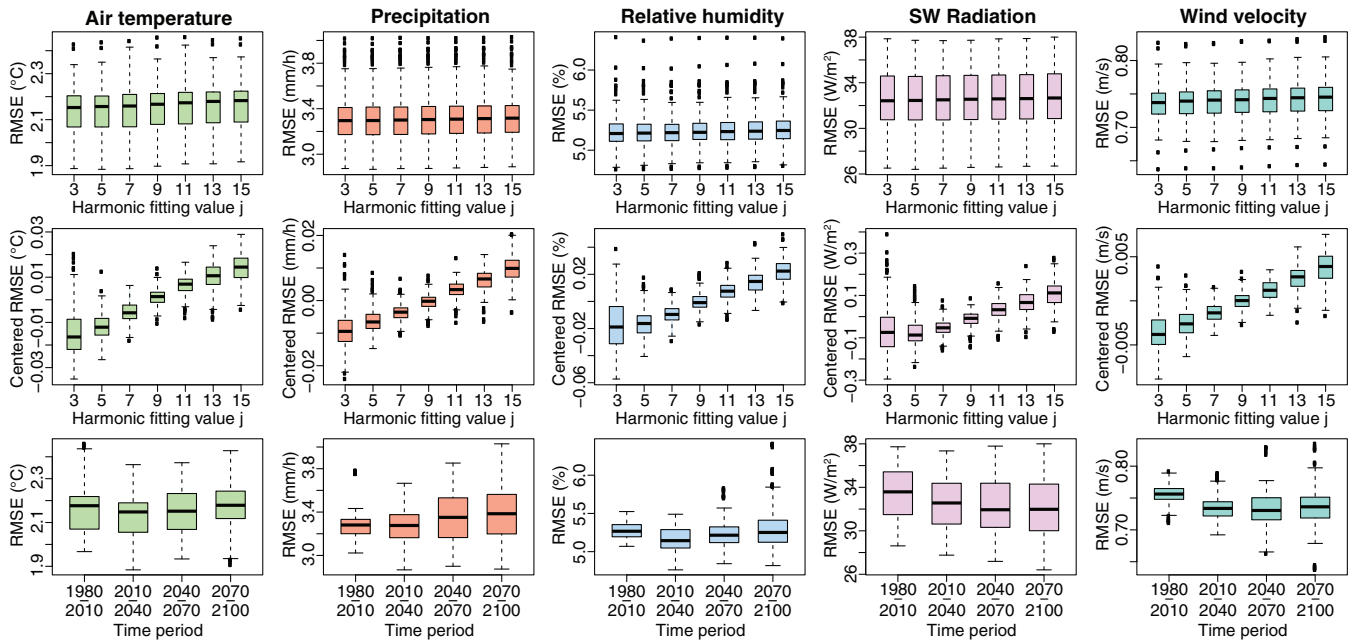


**FIGURE 8** Top row: Mean RMSE obtained using the method presented in Bosshard *et al.* (2011), applied to all CH2018 model chains and all four 30-years time periods for various values of  $j$ . Middle row: Centred mean RMSE, that is, same output as top row but for each model chain and variable the mean of the RMSE for all  $j$  value is subtracted separately, to remove the inter-model chain variability. Bottom row: Same as top row, but data sorted by downscaling period. Figure for the station Payerne [Colour figure can be viewed at [wileyonlinelibrary.com](http://wileyonlinelibrary.com)]

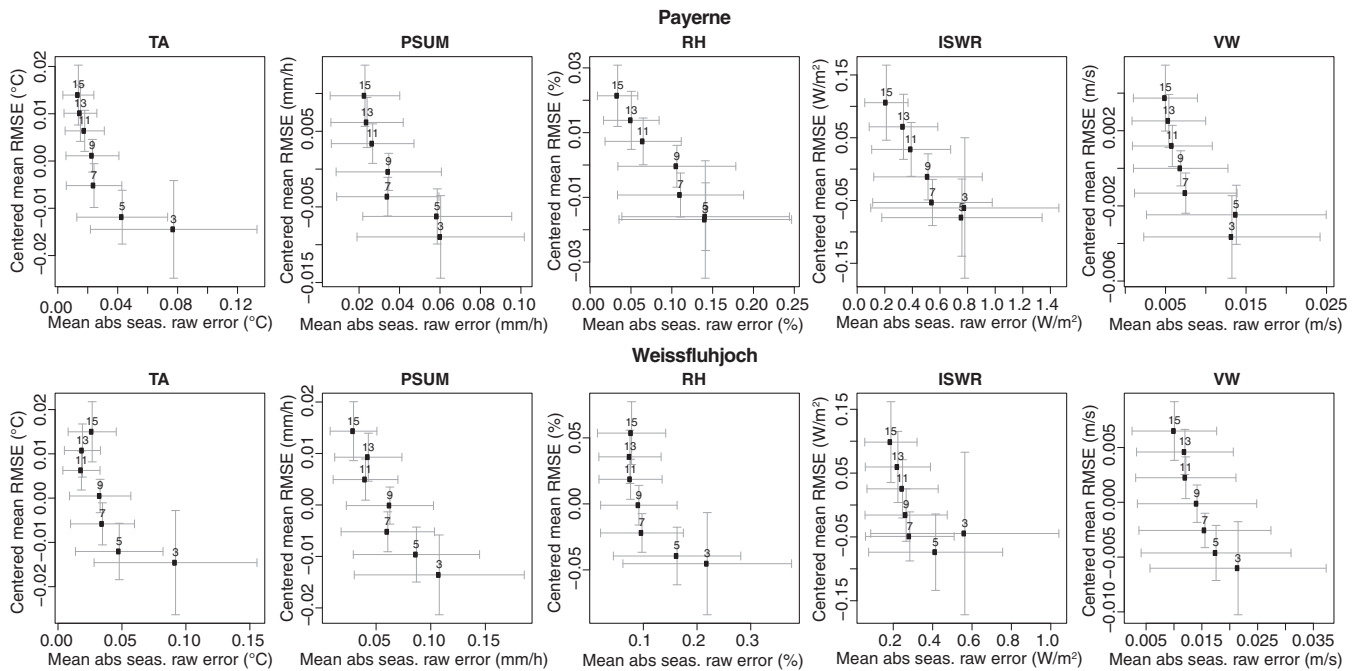


**FIGURE 9** Centred mean RMSE plotted against mean absolute seasonal raw error for all model chains and all time periods for the station Payerne. The numbers indicate the value of  $j$ , that is, the number of terms considered in the harmonic fitting

details are given in MeteoSuisse *et al.* (2018a), section 5.7. The present section also discusses further limitations arising from the temporal downscaling method used in this work.

The quantile mapping method used in CH2018 is calibrated over a historical time period and the correction function obtained is constant over time, meaning that the model bias is assumed to be constant over time. This

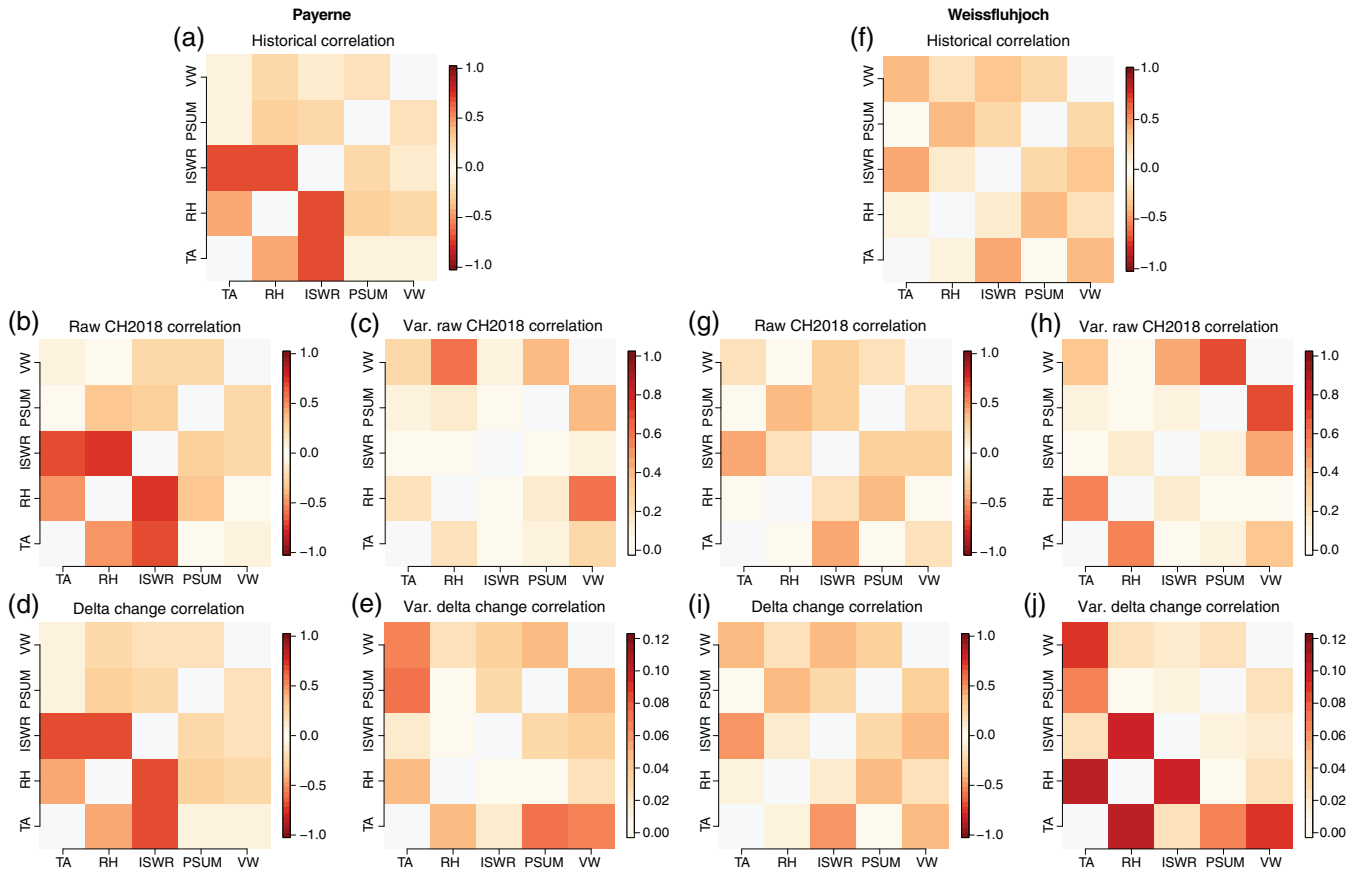


**FIGURE 10** Correlation between variables at the station Payerne (left) and Weissfluhjoch (right) for observed historical time series (top row), for raw CH2018 time series (middle row first and third plot) and for temporally downsampled time series (bottom row first and third plots). Second and third row use data from the 68 available scenarios. Second and fourth plots on second and third row show the variance of the correlation values between the 68 scenarios, note the change of scale between the second and third row in order for the correlation of the delta change time series to be visible. All correlations are computed using the period 1980–2010 [Colour figure can be viewed at [wileyonlinelibrary.com](http://wileyonlinelibrary.com)]

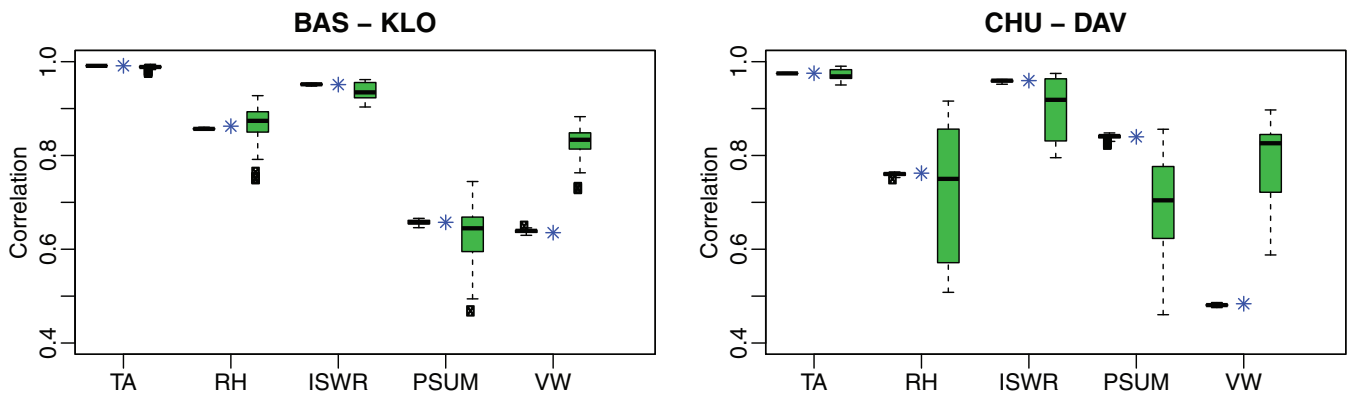


**FIGURE 11** Correlation between stations for the five variables used. Left: For the pair Basel Binningen – Zürich Kloten. Right: For the pair Chur – Davos. Blue stars show the correlation obtained from observations, black boxes show the correlation obtained from temporally downsampled CH2018 time series, and green boxes show the correlation obtained from raw CH2018 time series. All correlations are computed using the period 1980–2010 [Colour figure can be viewed at [wileyonlinelibrary.com](http://wileyonlinelibrary.com)]

assumption is uncertain because of multi-decadal climate variability. In addition, some statistical artefacts induced by quantile mapping, such as change in elevation

dependence of the warming rate, have been identified. The spatial climate variability at small scale, which is not present in RCMs outputs, might be not completely

captured by the quantile mapping. The complex topography of Switzerland might also cause the output of RCMs to be not representative of the meteorological stations in some pixels. Finally, large scale bias in GCMs or RCMs will not be corrected by quantile mapping and are still present in the CH2018 outputs. All these limitations add some uncertainty to the quantile-mapped time series. These limitations remain in the downscaled time series provided here and users should be aware of it.

Another limitation of CH2018 concerns possible changes in future extreme events. Quantile mapping might fail to correct bias for future extreme values lying outside of the range of historical values, leading to wrong intensities for extreme events in future climates. The method used in this work leads to a situation even worse for extreme events. The delta-change method only scales the intensity of the time series, and not the frequency of events in the data. This is important especially for precipitation, where the scaling might lead to unrealistically high precipitation extremes or to precipitation events that will actually not happen in a future dryer climate. As a consequence, the provided time series are not suited for use in the analysis of extreme events.

The fact that only intensity is scaled might likewise lead to unrealistic high shortwave solar radiation values. Potential decrease in cloudiness in climate change scenarios are not visible in the temporally downscaled time series (i.e., the period of time when solar radiation is below its theoretical maximum for clear sky at this time of the day does not change), but the whole time series is scaled up, meaning a brighter sun during clear sky periods and more transparent clouds. The opposite occurs in case of a decrease in incoming shortwave radiation in the CH2018 time series. The same applies for the scaling of relative humidity (which can be superior to 1) and of the wind speed. Depending on the application, users must apply appropriate filtering and correction to the data especially regarding upper bound values.

One inherent drawback of the method presented is the absence of transient time series. That is, only snapshots for the future are provided with discontinuities between them. In addition, the climate change signal in the time series is the mean signal over the whole period and the non-stationarity of the time series is driven by historical data only. In addition, sub-daily cycles are climate change agnostic in the downscaled time series, that is, they are the same as in historical time series. This should be considered as an additional source of uncertainty.

In summary, the method proposed for temporal downscaling is suited for use in models requiring hourly data as input, while only some parts of the climate change signal, that is, the monthly/seasonal to annual signal, is captured. All other effects arising from changes

in the frequency of events or from changes in short-term cycles are not captured and should be accounted for in the overall uncertainty. In addition, the obtained downscaled data set is not suited for studies of extreme events and the various sources of uncertainty mentioned in this section need to be accounted for.

## 5.2 | Usage of 10 years time series

The downscaled time series are provided over 10 and 30 years time periods for MCH station, and only over 10 years for IMIS stations. The usage of 10 years is appropriate when long enough historical time series do not exist to apply the temporal downscaling over 30 years. The usage of such shorter time series raises two questions: Is it representative to use only 10 years time series in impact studies, and is the downscaling method able to capture the delta correctly over 10 years only? Regarding representativeness, most climate change studies use 30 years periods, as recommended by the World Meteorological Organization (WMO, 2017). However, the same recommendations state that for most applications shorter time series, for example, 12 or 10 years, are also suited. The biggest concern of using 10 years time series is precipitation. Indeed, precipitation time series exhibit variations driven by long-term oscillations of the climate system (usually longer than 30 years). In the delta-change approach, the mean seasonal cycle from future time series is mapped to historical data. Therefore, all downscaled time series exhibit the same underlying inter-annual behaviour driven by large-scale atmospheric oscillation present in the historical time series. Looking at the difference between model outputs in the past and in the future only allows for assessing the impact of the main climate change signal while omitting parts of the perturbation from large-scale atmospheric oscillations and their potential future changes.

For answering the question concerning the ability of the delta-change method to capture the main annual signal over 10 years only, further investigations are required as this is a non-trivial problem. Performing an assessment similar to Section 4 is not possible. Indeed, comparison of time series downscaled over 10 and 30 years will probably show some differences, but it is impossible to identify whether: the cause of this is the inability of the method to capture the main behaviour of the time series over 10 years only, it is caused by a possible underlying trend in the historical data, or it is caused by some long-term oscillation not captured over 10 years. To avoid this pitfalls, stationary time series are required.

Stationary time series are obtained by using the one-dimensional weather generator AWE-GEN (Fatichi *et al.*, 2011). In this example, 500 realizations are generated

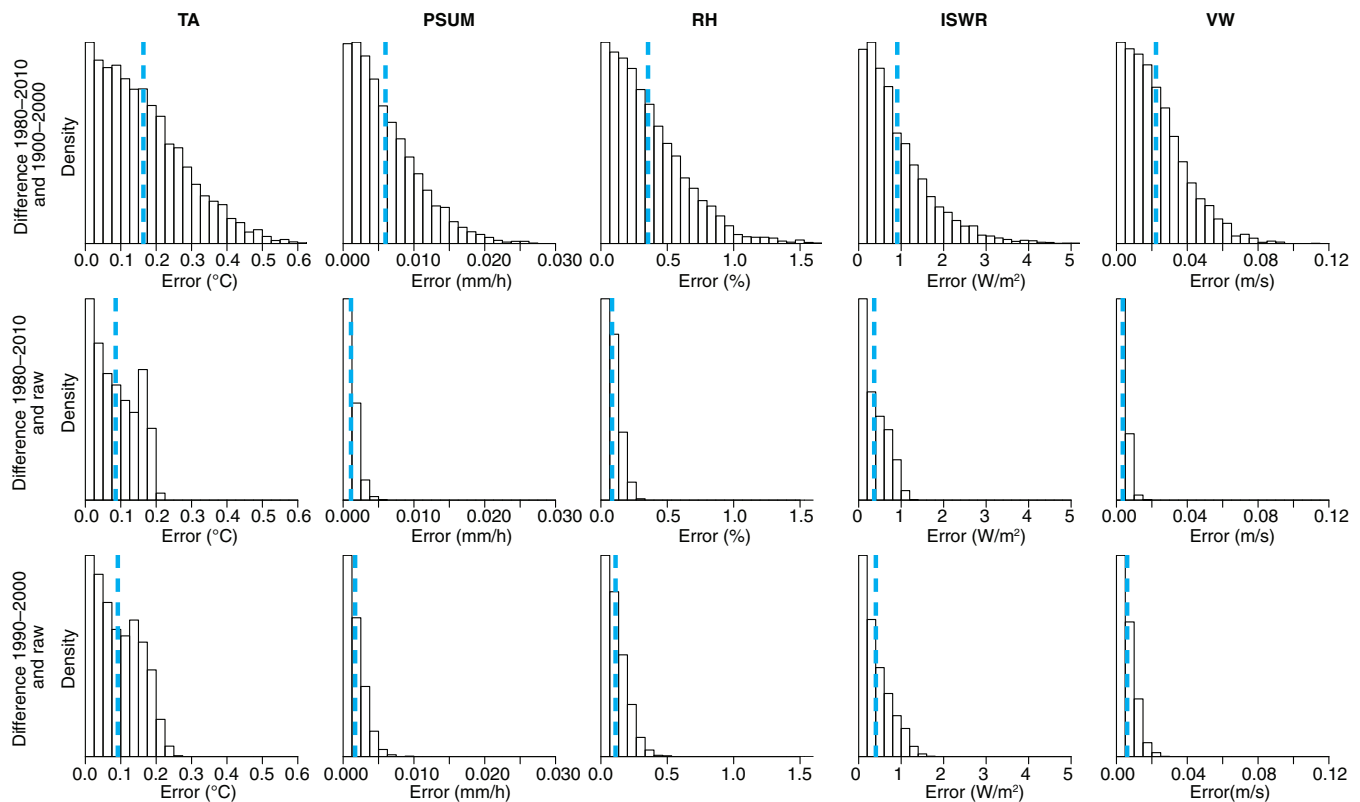


**FIGURE 12** Distribution of error in the seasonal mean of smoothed time series computed for 500 realizations of the AWE-GEN weather generator for the location Florence, Italy, with  $j = 7$ . First row: Error between time series smoothed over the period 1990–2000 compared to time series smoothed over the period 1980–2010. Second row: Error between time series smoothed over the period 1980–2010 compared to raw data over the same period. Third row: Error between time series smoothed over the period 1990–2000 compared to raw data over the same period. Blue dashed lines represent the mean values [Colour figure can be viewed at [wileyonlinelibrary.com](http://wileyonlinelibrary.com)]

for the location of Firenze in Italy over the 1980–2010 time period with inter-annual variation enabled in the generator. While additional variables are provided by the weather generator, only the same five variables as provided in CH2018 are used. For all the realizations, the time series are first DOY averaged and then smoothed using  $j = 7$  as smoothing parameter (Section 3). This procedure is performed over the whole 30 years time series, and also separately for each of the three decades. The seasonal mean of the time series smoothed over 10 and 30 years are computed and compared to the seasonal mean of the raw generated time series.

The results of this analysis are shown in Figure 12. There is a clear difference between the seasonal means obtained when using 10 or 30 years time series (first line of the figure). However, this does not tell whether the difference is due to the inter-annual variability present in the data (as discussed at the beginning of this section), or because the smoothing over a shorter time period is not able of capturing the mean seasonal signal. Panels in second and third rows of Figure 12 show seasonal means of smoothed time series compared to seasonal means of raw time series for 10 and 30 years. When using the 10 years time series, the error on seasonal means is slightly higher

and the distribution more spread than that found when using 30 years, but the differences are relatively small. Thus it can be concluded that the method itself is still robust when applied to the 10 years time series.

For all the time series provided together with this paper, we consider the uncertainties discussed in this section not important enough to forbid the usage of the 10 years downscaling product. Indeed, using decadal time periods allows for performing the downscaling over the whole IMIS station network resulting in a completely new data set of climate change scenarios over the Swiss alpine regions. When using only MCH time series, 30 years should be preferred; however, when a mix of MCH and IMIS stations is desired, 10 years time series should be used for both. In all cases, the 10 years time series should be used with caution and users should ensure that the product is suited for the purpose.

## 6 | CASE STUDY

In this section, a brief case study performed with the SNOWPACK model (Lehning *et al.*, 2002) is presented.

In Switzerland, many studies focus on the future evolution of the seasonal snow cover due to its importance for hydrology, electricity production and tourism. Some of these studies need to perform temporal downscaling of climate change scenarios to run the respective impact models. We show here the importance of correctly assessing the quality of these time series before application for such studies.

The model SNOWPACK is run for 10 MCH stations at high altitude using 30 years time series for the periods 1980–2010, 2010–2040, 2040–2070, and 2070–2100, and for 17 IMIS stations representative of the Alps for the periods 1990–2000, 2020–2030, 2050–2060, and 2080–2090. The model is run for all climate scenarios and all odd smoothing values  $j$  between 3 and 15, leading to a total of 35'532 model runs.

Two variables are extracted from the model output: The daily mean snow height, and the occurrence of rain on snow (ROS) events. They are defined here based on the work of Würzer *et al.* (2016): a ROS event is occurring when at least 20 ~ mm of rain fall within 24 ~ hr on a snow cover of at least 25 ~ cm at the onset of rain. From these three variables, five values of interest are extracted.

- ROS: The number of ROS events during the simulation period.
- HS<sub>5</sub>: The mean annual number of days when the snow height is greater or equal to 5 ~ cm.
- HS<sub>30</sub>: The mean annual number of days when the snow height is greater or equal to 30 ~ cm.
- HS<sub>Mean</sub>: The mean snow height for the months December–January–February (DJF) over the simulation period.
- HS<sub>Max</sub>: The maximum snow height reached over the simulation periods.

These values are then grouped by station, RCP,  $j$  values, and period, to obtain a distribution of values with one point per scenario. The distributions for various  $j$  values are then compared to see if they significantly differ. This difference is assessed using a two sided  $t$ -test assuming paired values and a significance level of .05. Figure 13 shows the proportion of such tests indicating a significant difference. Only the proportion of significant difference between the couple  $j \in (3, 7)$ ,  $j \in (3, 15)$ , and  $j \in (7, 15)$  are shown. In the first column the results are sorted by stations, and in the second column they are sorted by time period. Since the significance value of 0.05 assumes that 5% of the test might lead to false positive, a line is shown at 5%. This would assume that the false positive rate is equally distributed between the categories. For an even more conservative approach, we compute for each  $j$ -couple the total number of  $t$ -test indicating a

difference and compare it to the 5% of the total number of tests performed for this  $j$ -couple (342 tests per  $j$ -couple, so the expected number of false positive is 17). These numbers are indicated in the figure legends.

Figure 13 shows that for all of the 5 quantities studied, the number of occurrences when the results differ is larger than the expected false positive rate. As expected, the number of different distributions is largest for the couple  $j \in (3, 15)$ . For HS<sub>5</sub>, HS<sub>30</sub>, there are more differences in the couple  $j \in (3, 7)$  than in the group  $j \in (7, 15)$ . HS<sub>5</sub> and HS<sub>30</sub> being mainly determined by the beginning and ending time of the snow season, this result is in agreement with Sections 4.1 and 4.3, where we show that the biggest difference in seasonal mean is between small  $j$  values. ROS and HS<sub>Max</sub>, on the other hand, are more impacted by the variability. Since the increase of variability is almost linear with increasing  $j$  (see Sections 4.4 and 4.3), no important difference between the couples  $j \in (3, 7)$  and  $j \in (7, 15)$  is observed. Regarding HS<sub>Mean</sub>, the fact that the number of significantly different outputs is greater than 0 only at MCH stations (except for one IMIS station) is explained by the lower snow height at these stations.

The right column of Figure 13 suggests that most of the results indicating a difference are obtained over the historical periods. This is explained by the fact that differences between scenarios for a given RCP grow with time, leading to wider distributions (see Figure 14). Increasing the background variability leads to less significant influence of varying  $j$ . However, since most studies analyse results by subtracting values of interest from past periods to values from future periods, this error will be propagated to all results.

In summary, this case study shows the impact of the smoothing value  $j$  in a concrete example, and demonstrates that a non-negligible part of the results can be significantly different, highlighting the need of correct assessment of the downscaled time series. This statistical significance does not tell, however, whether the conclusion drawn on a real impact study would be different. Figure 14 shows the example of an obvious difference. This is probably a 'worst-case' scenario, but it is informative about the potential impact of different downscaling parameter values.

## 7 | CONCLUSION

In the present work, the delta-change approach used in the context of temporal downscaling of climate change scenarios was analysed in detail. The different steps required for obtaining downscaled time series are explained and justified. In particular, it is shown that a



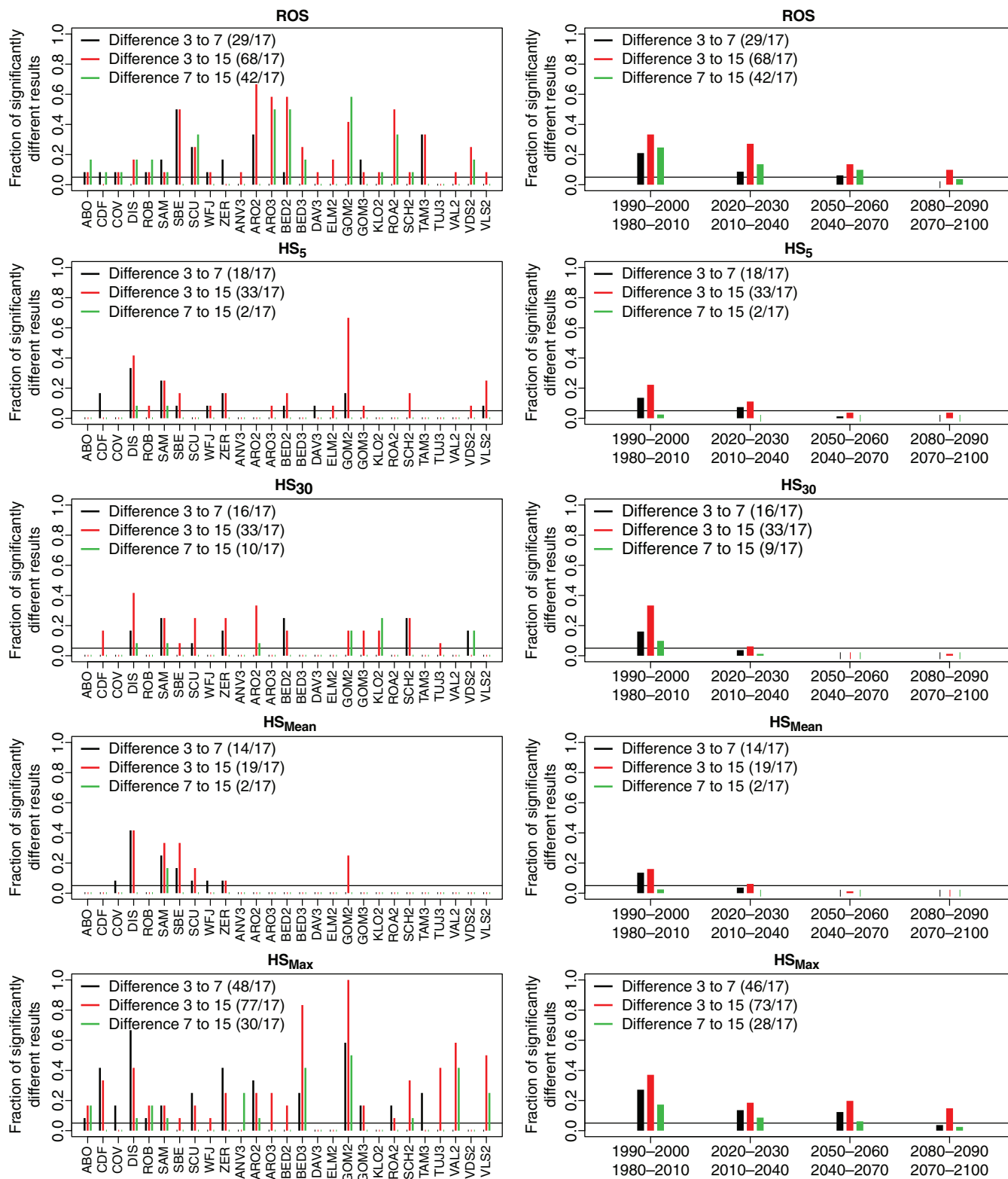


**FIGURE 13** Fraction of significantly different distribution of outputs of SNOWPACK models runs. Each distribution is composed of all model outputs for a given station, time period, variable and RCP. Distributions obtained with different values of  $j$  are compared and the fraction of significant difference (determined by a  $t$ -test) between two values of  $j$  is shown. Horizontal black lines show the 5% value, the expected rate of false positive. Numbers in the legend indicate the total number of positive tests and the total number of false positives expected [Colour figure can be viewed at [wileyonlinelibrary.com](http://wileyonlinelibrary.com)]

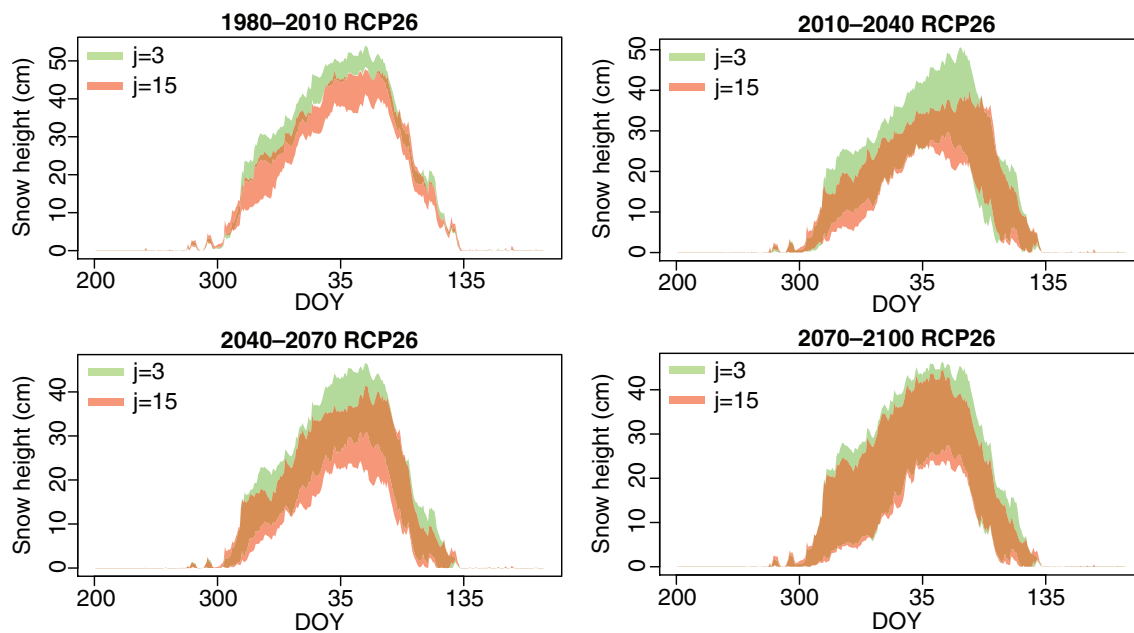


**FIGURE 14** Snow height simulated by SNOWPACK averaged for each DOY over the 30 years simulation periods at the MCH station Samedan (GR) Switzerland for RCP2.6. Forcing data are downscaled with  $j = 3$  (green) and  $j = 15$  (red). Significant difference in snow height (about 20%) can be observed for the first 3 time periods. The growing spread of the output in the future is explained by the growing difference between the climate change scenarios [Colour figure can be viewed at [wileyonlinelibrary.com](http://wileyonlinelibrary.com)]

smoothing of the historical and future time series is required and that the parameters chosen for this smoothing have a determinant impact on the correctness of the seasonal means of the downscaled time series as well as on the amount of artificial variability.

Using the CH2018 data set and the spatial transfer of this data set on the Inter-cantonal Measurement and Information System (IMIS) station network, it is shown that the smoothing parameter used in Bosshard *et al.* (2011) and in many other studies in Switzerland leads to sub-optimal results for the data sets used. A specific example of studying snow depth and rain on snow events using the SNOWPACK model showed significant difference in results obtained depending on the smoothing parameter used.

In order to get the best value for the smoothing parameter, we propose a new step-by-step two-factor assessment method based on the correctness of seasonal means and on the change in the natural variability induced by the downscaling. In addition to the detailed description of the method, source code is provided to perform such an analysis. The proposed method can be also applied with smoothing approaches different to the harmonic fitting used in this work. Application of this assessment on the two data sets used in this study (MeteoSwiss, MCH, meteorological data and IMIS snow and meteo data) shows that the use of seven harmonics for the smoothing of the input data was the best choice of

this parameter. However, this value corresponds to the data set used in this study and when applying the downscaling to a new data set, the assessment should be repeated to determine the best parameter for that specific case.

The method could be adapted to obtain transient delta and consequently transient time series, but it would require a de-trending of the observational time series. The development of a correct and robust assessment of the quality of the downscaled time series would be a major effort, though. Nevertheless, we do encourage the development of such an improvement and the code provided along with this study may provide a solid point of departure.

The quantile mapping used for the spatial downscaling of CH2018 is shown to break the correlation between variables measured at one individual site but also to break the observed correlation between nearby stations. The new delta method presented here allows for restoring this correlation which is an important prerequisite in physical models. On the other hand, the delta approach has a limitation concerning changes in the frequency of intermittent time series such as precipitation, prohibiting the use of the downscaled time series for studies of extreme events.

The application of the downscaling to the CH2018 and IMIS station networks also leads to the introduction of a new data set of climate change scenarios over

Switzerland. Ten-years hourly time series for 72 MCH stations and 116 IMIS stations for all decades between 1980 and 2,100, and 30 years time series for 58 MCH stations for the periods 1980–2010, 2010–2040, 2040–2070, and 2070–2,100 have been produced, released and are publicly available. These time series offer new opportunities to run physical models, especially over the alpine regions of Switzerland. This data set is actively used in the framework of the CH2018 (FOEN, 2018) and CCAMM (CCAMM, 2019) projects. As any climate change scenarios, they must be used with caution as detailed in Section 5.1, especially the 10 years time series. The main limitations are the incapacity to reproduce changes in future extreme events' frequency and amplitude, the absence of change in future sub-daily cycles, and the fact that these time series are not transient, but only slices of future time periods with discontinuities in between. Despite these limitations, the released product opens new perspectives for numerous impact studies in the alpine environment.

## DATA AND CODE AVAILABILITY

The data produced in this work, that is, the climate change daily time series obtained from QM at IMIS stations and the downscaled hourly time series are available at: <https://www.envidat.ch/dataset/climate-change-scenarios-at-hourly-resolution> and should be cited as: Michel, A., Sharma, V., Lehning, M., & Huwald, H. (2021). Dataset for: Climate change scenarios at hourly time-step over Switzerland from an enhanced temporal downscaling approach. EnviDat. doi: 10.16904/envidat.201.

The code used to perform the downscaling and to extract data from downscaled time series in order to assess the quality is available at: <https://www.envidat.ch/dataset/source-code-climate-change-scenarios-at-hourly-resolution> and should be cited as: Michel, A., Sharma, V., Lehning, M., & Huwald, H. (2021). Source code for: Climate change scenarios at hourly time-step over Switzerland from an enhanced temporal downscaling approach. EnviDat. doi: 10.16904/envidat.203β.

## ACKNOWLEDGEMENTS

The Federal Office of Meteorology and Climatology (MeteoSwiss) and the Swiss Institute for Snow and Avalanche Research (SLF) are acknowledged for the free access to their meteorological data. Petra Schmockler-Fackel and Fabia Hüsler from the Swiss Federal Office of Environment are sincerely acknowledged for their support. The authors thanks Sven Kotlarski and Jan Rajczak for helpful exchange during the elaboration of this work and in particular for making available their QM code used in Rajczak

*et al.* (2016) and for the production of the CH2018 data sets. The code is publicly available with GPLv3 licence at Kotlarski (2019). Finally, the authors thanks Radan Huth, Nadav Peleg, and an anonymous reviewer for their constructive and instructive comments during the revision process, and the International Journal of Climatology Editorial Office for their technical help. All analysis was performed with open and free software (Python and R), and the authors acknowledge the open-source community for its valuable contribution to science. This research has been supported by the Swiss Federal Office for the Environment (grant no. 15.0003.PJ/Q102-0785). This research was conducted in the framework of the FOEN program Hydro-CH2018 and in the framework of the WSL program Climate Change and Alpine Mass Movements.

## CONFLICT OF INTEREST

The authors declare no potential conflict of interest.

## AUTHOR CONTRIBUTIONS

Adrien Michel: Designed the study, collected the data and performed the temporal downscaling and its assessment. Main writer of the paper. Varun Sharma: Performed the spatial transfer for IMIS stations. Contributed to design the study. Contributed to write the paper and gave critical feedback. Hendrik Huwald and Michael Lehning: Contributed to design the study. Contributed to write the paper and gave critical feedback.

## ORCID

Adrien Michel  <https://orcid.org/0000-0001-9629-1989>

## REFERENCES

- Anandhi, A., Frei, A., Pierson, D.C., Schneiderman, E.M., Zion, M. S., Lounsbury, D. and Matonse, A.H. (2011) Examination of change factor methodologies for climate change impact assessment. *Water Resources Research*, 47.W03501.
- Bosshard, T., Kotlarski, S., Ewen, T. and Schär, C. (2011) Spectral representation of the annual cycle in the climate change signal. *Hydrology and Earth System Sciences*, 15, 2777–2788. <https://www.hydrol-earth-syst-sci.net/15/2777/2011/>.
- CCAMM (2019) *Climate change impacts on alpine mass movements*. <https://ccamm.slf.ch/en/general-overview.html>.
- CH2011 (2011) *Swiss Climate Change Scenarios CH2011*. published by C2SM, MeteoSwiss, ETH, NCCR Climate, and OCC, Zurich, Switzerland.
- Fatichi, S., Ivanov, V.Y. and Caporali, E. (2011) Simulation of future climate scenarios with a weather generator. *Advances in Water Resources*, 34, 448–467.
- FOEN (2018) Hydro-ch2018. <https://www.bafu.admin.ch/bafu/en/home/topics/water/info-specialists/state-of-waterbodies/state-of-watercourses/water-flow-and-flow-regime-in-watercourses/climate-change-and-hydrology/hydro-ch2018.html>.
- IDAWEB (2019) *Meteoswiss, federal office of meteorology and climatology*. <https://gate.meteoswiss.ch/idaweb/>.

- IMIS (2019) *Wsl institute for snow and avalanche research, slf, imis measuring network*. <https://www.slf.ch/en/avalanche-bulletin-and-snow-situation/measured-values/description-of-automated-stations.html>.
- Kotlarski, S. (2019) Sven kotlarski/qmch2018:qmch2018 v1.0.1. <https://doi.org/10.5281/zenodo.3275571>.
- Lehning, M., Bartelt, P., Brown, B., Fierz, C. and Satyawali, P. (2002) A physical snowpack model for the swiss avalanche warning: part ii. Snow microstructure. *Cold Regions Science and Technology*, 35, 147–167. <http://www.sciencedirect.com/science/article/pii/S0165232X02000733>.
- Maraun, D. (2016) Bias correcting climate change simulations – a critical review. *Current Climate Change Reports*, 2, 211–220. <https://doi.org/10.1007/s40641-016-0050-x>.
- Maraun, D., Shepherd, T.G., Widmann, M., Zappa, G., Walton, D., Gutiérrez, J.M., Hagemann, S., Richter, I., Soares, P.M.M., Hall, A. and Mearns, L.O. (2017) Towards process-informed bias correction of climate change simulations. *Nature Climate Change*, 7, 764–773. <https://doi.org/10.1038/nclimate3418>.
- MeteoSuisse, ETHZ, UNIBE and nat, S. (2018a) *CH2018 – Climate Scenarios for Switzerland, Technical Report*. Zurich: National Centre for Climate Services.
- MeteoSuisse, ETHZ, UNIBE and nat, S. (2018b) *Ch2018 – Climate scenarios for switzerland*. Zurich: National Centre for Climate Services. <http://www.ch2018.ch/en/home-2/>.
- Peleg, N., Fatichi, S., Paschalis, A., Molnar, P. and Burlando, P. (2017) An advanced stochastic weather generator for simulating 2-d high-resolution climate variables. *Journal of Advances in Modeling Earth Systems*, 9, 1595–1627. <https://agupubs.onlinelibrary.wiley.com/doi/abs/10.1002/2016MS000854>.
- Peleg, N., Molnar, P., Burlando, P. and Fatichi, S. (2019) Exploring stochastic climate uncertainty in space and time using a gridded hourly weather generator. *Journal of Hydrology*, 571, 627–641. <http://www.sciencedirect.com/science/article/pii/S0022169419301465>.
- Rajczak, J., Kotlarski, S., Salzmann, N. and Schär, C. (2016) Robust climate scenarios for sites with sparse observations: a two-step bias correction approach. *International Journal of Climatology*, 36, 1226–1243. <https://rmets.onlinelibrary.wiley.com/doi/abs/10.1002/joc.4417>.
- Storch, H.v. and Zwiers, F.W. (1999) *Statistical Analysis in Climate Research*. Cambridge: Cambridge University Press.
- Taylor, K.E., Stouffer, R.J. and Meehl, G.A. (2012) An overview of CMIP5 and the experiment design. *Bulletin of the American Meteorological Society*, 93, 485–498. <https://doi.org/10.1175/BAMS-D-11-00094.1>.
- WMO (2017) *WMO Guidelines on the Calculation of Climate Normals*. Tech. rep., World Meteorological Organization.
- Würzer, S., Jonas, T., Wever, N. and Lehning, M. (2016) Influence of initial snowpack properties on runoff formation during rain-on-snow events. *Journal of Hydrometeorology*, 17, 1801–1815. <https://doi.org/10.1175/JHM-D-15-0181.1>.

## SUPPORTING INFORMATION

Additional supporting information may be found online in the Supporting Information section at the end of this article.

**How to cite this article:** Michel A, Sharma V, Lehning M, Huwald H. Climate change scenarios at hourly time-step over Switzerland from an enhanced temporal downscaling approach. *Int J Climatol*. 2021;1–20. <https://doi.org/10.1002/joc.7032>